We are IntechOpen, the world's leading publisher of Open Access books Built by scientists, for scientists

4,800
Open access books available

122,000
International authors and editors

135M
Downloads

Our authors are among the

154
Countries delivered to

TOP 1%
most cited scientists

12.2%
Contributors from top 500 universities

CLARIVATE ANALYTICS BOOK CITATION INDEX INDEXED

WEB OF SCIENCE™

Selection of our books indexed in the Book Citation Index in Web of Science™ Core Collection (BKCI)

Interested in publishing with us?
Contact book.department@intechopen.com

Numbers displayed above are based on latest data collected.
For more information visit www.intechopen.com

Chapter

Aluminum Alloys Behavior during Forming

Perumalla Janaki Ramulu

Abstract

Industrial revolution toward weight reduction and fuel efficiency of the automotive and aerospace vehicles is the major concern to replace heavy metals with light weight metals without affecting much strength. For this, aluminum alloys are the major contributors to those industries. Moreover, aluminum alloys are majorly categorized as 1xxx, 2xxx, 3xxx, 4xxx, 5xxx, 6xxx, 7xxx, and 8xxx based on major alloying elements. Among all, 2xxx, 5xxx, 6xxx, and 7xxx are having majority of applications in the abovementioned industries. For manufacturing any engineering deformable components, forming characteristics are must. Forming behavior of aluminum alloys has been evaluated through different processes including deep drawing, stretching, incremental forming, bending, hydro forming etc., under different process conditions (cold, warm, and hot conditions) and process parameters. Each process has its own process feasibility to evaluate the formability without any forming defects in products. The present chapter discusses a few important processes and their parameter effect on the aluminum alloys through the experimentations and simulation works.

Keywords: ISF, hot forming, tube hydroforming, deep drawing, stretching

1. Introduction

Formability is defined as plastic deformation ability to produce a part with definite requirements on mechanics, dimension, and appearance of a material during a forming process, being mainly limited by the occurrence of flow localization or variability. The formability of any sheet material depends on the material properties, process parameters, and strain bounding criteria. The formability can be evaluated through simulation tests like stretching, deep drawing and drawing processes, mechanical tests, limiting dome height (LDH), and forming limit diagrams at various conditions. Evaluating the formability of aluminum alloys is crucial for industries like aerospace and automotive due to their significant advantages over other materials. Aluminum alloys are majorly categorized as 1xxx, 2xxx, 3xxx, 4xxx, 5xxx, 6xxx, 7xxx, and 8xxx based on major alloying elements. Among all, 2xxx, 5xxx, 6xxx, and 7xxx are having majority of applications in any industry. Forming behavior of aluminum alloys has been evaluated through different processes including deep drawing, stretching, incremental forming, bending, hydroforming, etc., under different process conditions (cold, warm, and hot conditions) and process parameters. Each process has its own process feasibility to evaluate the formability without any forming defects in products. The significance of this chapter is to discuss and elaborate the effect of forming process parameters of different

processes on various aluminum alloys. Specifically, the hot forming process, deep drawing process, incremental forming process, tube hydroforming process, and stretching process are discussed on different aluminum alloys.

2. Aluminum alloy behavior during hot forming

Hot forming of aluminum alloys is extensively used in the modern industry and has been explored by many researchers and scientists. The main intension to derive this process is to reduce in-flow stress, increase ductility, reduce work hardening, increase toughness of the material, etc. Furthermore, temperatures lower than those involved during hot forging make easier the obtaining of close tolerances and high surface finish [1]. To lead the hot forming process on different aluminum alloys, different process parameters were considered and the attachable results to the literature were derived.

For details, high-temperature tensile deformation of AA 6082-T4 was experimented in the temperature range of 623–773 K at several strain rates in the range of 5×10^{-5} to 2×10^{-2} s^{-1}. By this, stress exponent n of 7 during the ranges of temperatures and strain rates was tested. This is higher than what is usually observed in Al-Mg alloys under similar experimental conditions. Improvement in the strain exponent of any material leads to better formability [2]. Hot compression tests were performed on aluminum alloys 7150 and 2026 by varying the temperature from 300°C to 450°C and at a strain rate from 0.01 s^{-1} to 10 s^{-1} [3, 4]. Also, on AA 7075-T6 and AA 7085 aluminum alloy [5, 6] tested at different temperatures and strain rates (450, 500, 520, 550, 580°C and 0.004, 0.04 and 0.4 s^{-1} for AA 7075 and AA 7085 in the temperature range from 250°C to 450°C and at strain rate from 0.01 s^{-1} to 10 s^{-1} using Gleeble-1500 system, whereas hot deformation behavior was studied on aluminum alloys consisting of Al–6.2Zn–0.70Mg–0.3Mn–0.17Zr with temperature range of 623–773 K and strain rate of 0.01–20 s^{-1} [7]. Using the metallographic and transmission electron microscope, structural changes were studied. The results showed that the true stress-true strain curves exhibit a peak stress at a critical strain, after which the flow stresses decrease monotonically until high strains. The peak stress level decreases with increasing deformation temperature and decreasing strain rate. Similarly, Ag-containing 2519 aluminum alloy hot deformation behaviors were studied by isothermal compression at 300–500°C with strain rates from 0.01 to 10 s^{-1}. Consequences indicated that by increasing the strain rate and decreasing the deformation temperature, the flow stress of the alloy increased. And also, at a strain rate lower than 10 s^{-1}, the flow stress increases with increasing strain until the stress reached the peak value, and later on, a constant flow stress was noted [8]. Aluminum alloy of grade 7075 sheets fabricated by twin roll casting and deformation behavior was investigated at high temperature. At high temperatures from 350 to 500°C and strain rates from 1×10^{-3} to 1×10^{-2} s^{-1}, hot tensile test was performed. The results showed that by increasing the strain rate and decreasing deformation temperature, flow stress was increased [9]. Similarly, three aluminum alloys containing different silicon contents were studied at a temperature range of 573–773 K with strain rates of 0.01, 0.1, 1 and 5 s^{-1} [10].

Hot deformation behavior using processing map technique of stir cast 7075 alloy was studied. Based on the values of a dimensionless parameter like an efficiency index of energy dissipation, mapping was understood in terms of microstructural processes. Under the temperature and strain rate conditions, the processing map exhibited one distinct domain without any unstable flow conditions. In the processing map, the dynamic recrystallization zone and instable zones were identified. The processing maps can be used to select optimum strain rates and temperatures for effective hot deformation of 7075 alloy [11].

Elevated temperature and strain rate were aimed by stamping of AA5083 sheet components. To evaluate mechanical properties and forming behavior, tensile and Nakajima-type tests were carried out. The material flow stress, ductility, and fracture limit sensitivity to temperature and strain rate were evaluated. And also, the optimal combination of process parameters for maximum formability and effective post-deformation mechanical properties were determined [12]. A special device was developed to investigate the hot forming-quenching integrated process of cold-rolled 6A02 aluminum alloy sheet. The strengthening effect was replicated by hardness and uniaxial tensile tests. Microstructure examination was also conducted to clarify the strengthening mechanism. Results showed that hardness increases with solution time increase, and improves significantly after artificial aging. The faster the cooling rate, the greater the strengthening effect. On the same alloy, hot forming-quenching integrated process at different temperatures from 50 to 350°C was investigated. Results showed that the Vickers hardness and tensile strength decreased with increasing forming-dies temperature. To obtain enough strengthening effect, the forming-dies temperature should not be more than 250°C [13].

Springback and microstructure of the final products were analyzed and mechanical properties of the material were measured by tensile tests. The results show that HFSC can improve the formability of AA2024 aluminum alloy. After natural aging for 96 h at room temperature, the products were subjected to the hot bending process with synchronous cooling exhibiting a significant increase in strength. Springback of the aluminum alloy AA5754 under hot stamping conditions was characterized under stretch and pure bending conditions. It was found that elevated temperature stamping was beneficial for springback reduction, at hot dies [14, 15]. Hot stamping was developed for aluminum alloy to improve formability and avoid thermal distortion by combining hot forming and quenching. The effects of heating temperature on formability and strengthening of a solution treated with Al-Mg-Si alloy sheet, uniaxial tensile test, deep drawing test, and free bulging test were carried out at temperatures ranging from 25 to 500°C. It was observed that when temperature was raised to 400°C, the fracture strain and limiting bulging height were increased, whereas the limiting drawing ratio increased as temperature elevated to 200°C and declined subsequently. The mechanical property hardness was changed by increasing temperature and at 200 and 500°C, two peak hardness values were noted. Enhanced formability and strength were obtained simultaneously at 200 and 500°C, either of which can be chosen as appropriate forming temperatures for hot stamping [16]. At different solution heat treatment (SHT) temperatures, SHT time and lubricant stamping experiments were performed with 6061 and 7075 aluminum alloy sheets to investigate the formability and lubrication off a B-pillar. After trimming precision level, forming detections were also carried out. From these observations, the B-pillar wrinkled badly and cracked or even broke into pieces in cold stamping with or without lubricants [17].

For AA 6061 tailor rolled blanks (TRBs), an integrated hot forming and heat treatment process was proposed to improve the formability and dimensional accuracy. The experimentation of this process for sheet forming of Al6061 TRB was evaluated by performing the Erichsen and V-bending tests. The integrated hot forming and heat treatment process was also compared with the conventional forming method in terms of formability, dimensional accuracy, and mechanical properties [18]. A hot AA6082 specimen and cold P20 tools were studied as a function of contact pressure, specimen thickness, and lubricant, using the inverse FE simulation method for the interfacial heat transfer coefficient (IHTC) evolutions. To predict IHTC evolutions with reductions of different lubricants of sliding distance at different contact pressures and sliding speeds as a function, an interactive model was developed. The interaction between the lubricant and IHTC was deducted such

that it had three stages such as stage I: the lubricant is applied excessively and the IHTC is plateaued, stage II: in which the lubricant diminishes during sliding and the IHTC decreases, and stage III: lubricant breakdown occurs and the IHTC is equal to its values under dry conditions [19].

3. Aluminum alloy behavior during deep drawing process

The drawing of metal or "deep drawing" is the process by which a punch force is applied to sheet metal to flow between the surfaces of a punch die. By this, the sheet is formed into cylindrical, conic, or box-shaped parts. The development of the deep drawing process has paralleled scientific development, particularly in the aircraft and automotive industries. This process is more popular because of its swift press cycle times. Complex axisymmetric geometries and certain nonaxisymmetric geometries can be produced with a few operations. With respect to the functional perspective, the deep drawing process produces high-strength and lightweight parts as well as geometries unattainable with some other manufacturing processes [20]. A schematic illustration of these deep drawing processes is shown in **Figure 1**. This design is made in such a way that thickness reduction of the workpiece material has been avoided completely (**Figure 1**). For this process, the basic tools are the punch, the drawing die ring, and the blank holder.

Figure 2 shows the important process parameters involved in the deep drawing process. In addition, material properties such as the strain hardening coefficient (n) and normal anisotropy (R) affect the deep drawing operation.

Instead of tool temperatures, forming temperature curves (FTCs) were characterized from AA5754-O as a workpiece temperature at the warm deep drawing (WDD) process. The distinctive behavior of these curves was examined under nonisothermal WDD of AA 5754-O. The process parameters were considered such as FTC, blank holder force, and punch velocity to assure deep drawability. Optimum conditions were investigated by evaluating the cup volume and spring-back parameters. In the findings, 330°C in the flange-die radius region and 100°C in the cup wall-punch bottom region were the ideal optimum temperatures for the warm deep drawing process [21]. The stress-strain response of AA2014, AA5052, and AA6082 aluminum alloys at four temperatures: 303, 423, 523 and 623 K, and three strain rates: 0.0022, 0.022, and 0.22 s^{-1} was evaluated through uniaxial tensile tests. It was found that the Cowper-Symonds model was not a robust constitutive model, and failed to predict the flow behavior. A comparative study was followed for modeling of three aluminum alloys under the mentioned strain rates and temperatures. For comparison, the capability of Johnson-Cook model, modified models

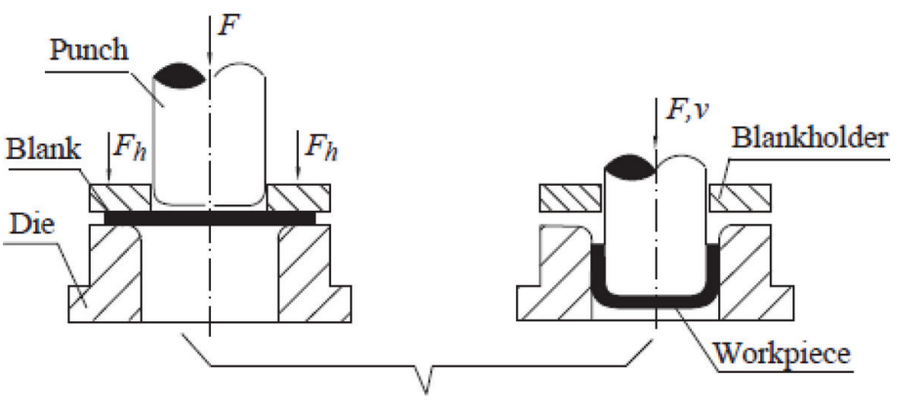

Figure 1.
Schematic illustration of deep drawing process [20].

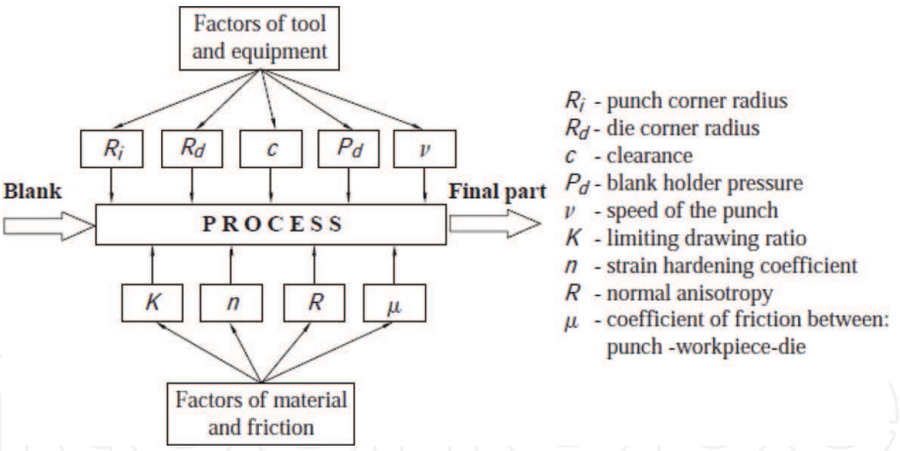

Figure 2.
Significant variables in deep drawing [20].

of Zerilli-Armstrong and Arrhenius and artificial neural network were considered for constitutive behavior. Better formability of the materials was observed at an elevated temperature of 623 K in terms of cup height and maximum safe strains by conducting cylindrical cup deep drawing experiments under two different punch speeds of 4 and 400 mm/min [22]. Tensile tests of AA5754-H22 aluminum alloy were carried out at five different temperatures and three different strain rates to investigate the deformation behavior correlating with the Cowper-Symonds constitutive equation.

When punch and die were heated to 200°C, the forming limit strain and dome height were improved. Significant enhancement was noted when the die and punch temperatures were maintained at 200 and 30°C, respectively, in deep drawn cup depth. Using a thermo-mechanical FE model, the forming behavior at different isothermal and nonisothermal conditions was predicted. In the FE model, temperature-dependent properties in Barlat-89 yield criterion and coupled with Cowper-Symonds hardening model were used. The validation had taken place using thinning/failure location in deformed cups by implementing the experimental limiting strains as damage model [23].

Deep drawing of aluminum alloy AA6111 at elevated temperatures was analyzed with the effect of friction coefficient through experiments and finite element method. Results indicated that the friction coefficient and lubrication position influence the minimum thickness, the thickness deviation, and the failure mode of the formed parts. During the hot forming process, the failure modes were draw mode, stretch mode, and equi-biaxial stretch mode. Fracture occurred at the center of cup bottom or near the cup corner in a ductile mode or ductile brittle mixed mode [24]. Simulations of deep drawing tests at elevated temperatures were carried out with experimental validation on aluminum alloy 7075. For stamping operations, some of the important parameters such as blank holder force, stamping speed, blank temperature, and friction coefficient were considered. During the experimentation, stamping tests were performed at temperature between 350 and 500°C, 0 and 10 kN blank holding force, 50 and 150 mm/s stamping speed, and 0.1 and 0.3 frictional coefficient. At lower values of temperature, blank holder force and friction coefficient improvement were seen in thickness homogeneity whereas formability was improved with the well lubricated blank at about 400°C temperature and stamping speed 50 mm s^{-1} [25]. Tailor friction stir welded blanks (TFSWBs) of AA5754-H22 and AA5052-H32 sheet metals were fabricated using a tool with optimized design along with optimized process parameters. For optimization to design the friction stir welding experiments, Taguchi L9 orthogonal array was used. For

the multi-objective optimization to maximize the weld strength and total elongation reducing the surface roughness and energy consumption, the gray relational analysis was applied. The formability was evaluated and compared with TFSWBs and parent materials using LDR tests. The analysis had proved that TFSWBs were comparable with parent materials more specifically without any failure in the weld zone area. For improvement in the LRD, a modified conical tractrix die was proposed and 27% improvement was observed.

Simulations of cylindrical cup drawing were carried out with experimental validation on AA6111 aluminum alloy at elevated temperatures. The influence of four important process parameters, namely, punch velocity, blank holder force (BHF), friction coefficient, and initial forming temperature of blank on drawing characteristics was investigated using design of experiments (DOE), analysis of variance (ANOVA), and analysis of mean (ANOM). Based on the results of ANOVA, the BHF had the greatest influence on minimum thickness. The significance of punch velocity for thickness deviation, BHF, friction coefficient, and initial forming temperature of blank was 44.35, 24.88, 15.77, and 14.995% respectively. Further, the effect of each factor on forming characteristics was analyzed by ANOM [26].

A design optimization problem was constructed to identify the formability window, in which the punch stroke was maximized subject to wrinkling and tearing. For this, the formability window of a difficult-to-draw material AA 5402 was explained with the pulsating blank holder force (PBHF) and the variable blank holder force (VBHF). Some parameters in the VBHF and PBHF were included and taken as the design variables. A sequential approximate optimization (SAO) using a radial basis function (RBF) network was used to determine the optimal parameter of PBHF and VBHF. From numerical simulation coupled with the SAO using the RBF network using the PBHF and VBHF, formability window was observed. It was identified that the proposed approach was highly useful for clarifying the formability window of a difficult-to-draw material [27]. The tailored heat treated blank (THTB) technique was demonstrated to create a material property gradient through a suitable artificial aging treatment carried out prior to the forming process on the effectiveness of combining the hydromechanical deep-drawing process. This method was coupled with a simple finite element model and a multi-objective optimization platform. For determining the effect of the aging treatment on the mechanical and deformative behavior of the AC170PX aluminum alloy, a preliminary experimental campaign was carried out. The adoption of aged blanks in the hydromechanical deep drawing allows to increase the limit drawing ratio and to simplify the process proved from the optimization results [28].

For increasing the drawability of AA1200 aluminum alloy cylindrical cups, one technique was developed. For optimal process design, effects of die and punch along with fillet radius of die and punch on LDR, drawing load with respect to punch stroke and strain of the cup wall was investigated numerically. To determine the optimum LDR form numerical analysis, a commercial finite element simulation package, ANSYS 14.0, was used. The effects of the original blank on the various LDR and punch load were numerically investigated. This process successfully produced cylindrical cups with considerable drawing ratio [29]. The effect of pulsating blankholder system was investigated on improving the formability of aluminum 1050 alloy. Using ABAQUS6.7 software, the deep drawing process was simulated for cylindrical cup of AA 1050. Later on, experimental and numerical analyses were compared for depth of cup, tearing, and thickness distribution. The results indicated that with proper frequency and gap, the cup depth and thickness distribution can be improved by using the pulsating blankholder system. Further, good agreement was observed between simulation and experimental results [30]. An analytical model was proposed for the nonuniform fluid pressure distribution

in the cavity and for the hydrodynamic flow of the fluid film between the blank and die for AA5086 aluminum alloy. From Reynolds equation solution, the hydrodynamic flow was calculated and model was implemented in ABAQUS/Explicit, finite element software. The approach was validated and investigated for the influences of the blank holder force and the fluid pressure on the formability of the blank metal. The results exhibited that the choice of an appropriate blank holder force reduced the strain in the blank and prevented the risk of fracture [31]. A study was made on deep drawing of SiCp/2024Al composite sheets by considering the effect of pulse current on heating performance and thermal. The high-intensity pulse current flows through the sheet and generates the tremendous Joule heat. The specimen temperature was kept around 673 K at a rate of 13.5 K/s under the current density of 21.7 A/mm^2. The temperature difference was reduced by 73.3% by inserting the stainless-steel inserts. Besides, the SiCp/2024Al composite was successfully deep drawn with good surface quality [32]. Deep drawing process characteristics of AA 6xxx alloy sheet were discussed under different process parameters such as punch force, lubrication, fillet radius, punch speed etc., and the formability was evaluated [33–37].

4. Aluminum alloy behavior during incremental forming

Incremental sheet forming (ISF) is a flexible process in which a sheet of metal is formed by a progression of localized deformation. This process does not require any specialized tool; a simple tool moves over the surface of the sheet metal by which localized plastic deformation is initiated. Hence, many shapes can be formed by designing a proper path to a tool. The main motto of this process is to form a sheet metal without any manufacturing of specialized dies [38]. **Figure 3** shows an example of the incremental forming. In this **Figure 3**, according to computer numerical control (CNC) machine program instructions, the ball tool moves on the sheet to form the required shape. Hence, the process is in CNC machine; the program can be edited as per the requirement. From the shown **Figure 3**, the hollow and square in cross section will be formed [39].

A few observations are made and discussed on incremental forming process. Incremental forming behavior of 6111-T4 an alloy was investigated for exterior body panel applications. Tensile testing data were used to simulate the incremental forming

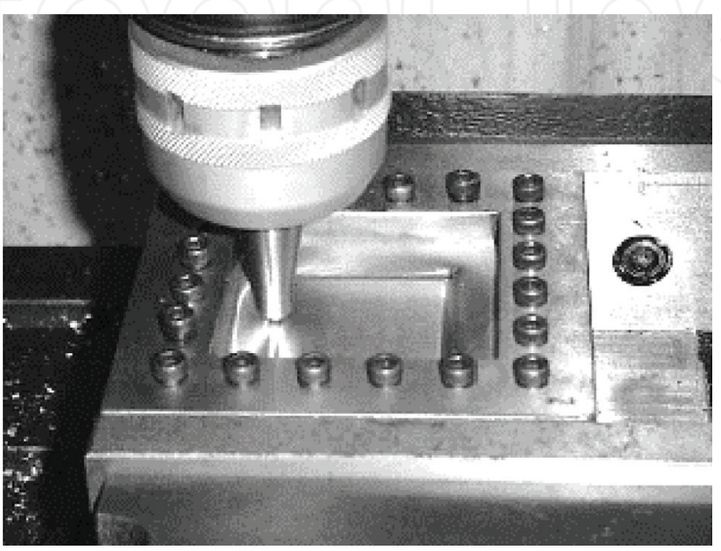

Figure 3.
Incremental forming of an aluminum sheet on CNC milling machine [34].

process. The heat treat regimen developed for uniaxial testing was then applied to a series of plane strain tests using a hemispherical punch [40]. The formability of AA-2024 sheets was investigated in the single-point incremental forming (SPIF) process. The process parameters, specifically step size, tool radius, and forming speed, of the SPIF process were varied over wide ranges. The formability was quantified through a response surface method. It was found that the interaction of step size and tool radius was very significant on the formability. The formability of pre-aged AA-2024 sheet decreases with the increase in the forming speed. Additionally, the annealed sheet shows higher formability than the pre-aged sheet [41].

AA7075-O aluminum alloy sheet forming was investigated using experimental campaign and the forming process mechanism was understood. Tensile tests were carried out to characterize the mechanical properties with three different thicknesses. To illuminate the formability of AA7075-O aluminum alloy sheet, the effects of tool path with different incremental steps and the part height were evaluated. To understand the design limits for strain, a fracture forming limit diagram was developed. The influence of different draw angles, sheet thicknesses, step-down sizes, and sheet orientations was considered to analyze forming forces. The part draw angle and incremental steps of the tool path were more effectible on the formability as concluded from the experimental results. The influences of process parameters on tool forces provide further insights into the deformation mechanics of AA7075-O sheets [42]. The formability of AA5052 aluminum alloy at room temperature was studied through truncated square pyramid and cone formed using a CNC machine. For both the shapes, the forming limit diagram (FLD) and thickness distribution were predicted and compared. The FLD obtained through this process and conventional FLD were different. Comparison of FLD and thickness distribution showed that cone had higher forming limit than square cup and the thickness after forming was better in cone shapes than in square cups [43]. An investigation was made on the deformation characteristic of embossed aluminum sheet in the incremental sheet forming process in which the surface quality of tool path along outward and inward movement was compared and noted as surface quality is better in the outward movement. Using ABAQUS software, a finite element simulation, the experimental results and detailed forming mechanism of the 3D structured sheet were reviewed [44].

Formability of friction welded blank made of aluminum 6061 was studied experimentally. Formability was evaluated through FLD, dome height, minimum thickness, and thickness distribution. Many experiments were conducted to know which joining direction caused higher formability and desired forming limit curve. Joints were prepared in three different rollings (0, 45, and 90°) and tested for formability test and compared with FLD, dome height, minimum thickness, and thickness distribution. From the formability comparison, the best joining direction was identified. Using the response surface methodology, the effect of welding process parameters such as rotational speed, plunge depth, and travel speed on formability of welded blanks was analyzed. After finding the effects, welded blanks with optimal parameter combination were fabricated and the effect of incremental forming parameters, that is, spindle speed, feeding rate, and axial step on thickness distribution was analyzed. From the results, it was obtained that joints with diagonal direction caused higher value of bowl height [45]. The effect of longitudinal ultrasonic vibrations on the performance of the incremental forming process of aluminum-1050 sheet was studied. In this technique, ultrasonic vibrations with high frequency and low amplitude were axially added to the movement of forming tool. This system is arranged with different parts including a mechanism attached into the chuck of CNC machine and ultrasonic power to the vibratory tool. Parameters like forming force and sheet formability were examined through straight groove

test in both conventional and ultrasonic-assisted incremental forming process. The results showed that formability increased and forming force decreased with ultrasonic assistance [46].

Using the finite element method, the behavior of the state of stresses and strains in the hot incremental sheet forming of 1050 aluminum alloy was evaluated, with and without pre-heating. With the assistance of RADIOSS software, numerical simulation was performed. The results were presented a deterioration in the force during electric hot incremental sheet forming compared to the electric hot incremental sheet forming [47].

The formability of the AA2024-O aluminum alloy sheet material was evaluated with respect to the impact of forming tool shape, tool diameter, wall angle, step size, sheet thickness, and tool rotation. Forming depth was measured by scanning the components using a noncontact 3D scanner. Wall angle and step size had proved more significant factors which affect the formability greatly [48]. An attempt was made to optimize the incremental forming parameters (spindle speed, tool feed, and step size) for surface roughness to be least and wall thickness to be larger using the response surface method.

The formability of AA5052 alloy sheets at room temperature was checked with pre-cut holes at the center with different diameters. In the forming operation, cone-shaped parts were formed with the optimized values. Formability was compared with sheet with smaller holes and larger holes and it was observed that smaller holes had better formability. Also, the thickness of the formed part wall without hole is less. As the diameter of the hole increases, the wall thickness also increases [49].

To evaluate deformation behavior of AA-6061 aluminum alloy sheet, the single point incremental forming (SPIF) process was chosen. To form the sheet into the desired conical shape, the SPIF experiments and finite element method simulation were performed and to measure the major and minor strains, the digital image correlation (DIC) method was used. The major and minor strains in post deformation results were compared with FEM results for AA6061 thin sheet material. An experimental fracture forming limit diagram was assessed using the punch stretching test.

Consequently, the effective plastic strains at the onset of fracture were predicted and compared with experimental data. In order to get insight into forming behavior and surface roughness, the microstructural examination on the truncated dome fabricated using optimized parameters was carried out through micro-texture analyses [50]. By using the electric hot incremental forming process (EHIF), the dimensional accuracy of parts has got more improvement compared to single-stage forming and double-stage forming at room temperature. The effect of EHIF process parameters, such as tool diameter, feed rate, step size, and current, on temperature was studied. For a cone of AA 1060, the maximum temperature, the average temperature, and the maximum temperature difference were measured. Besides, the response surface method and Box–Behnken design were employed, and they established corresponding models to predict targeted values [51].

AA 7075-O sheets were formed into variable angle funnels and 45° wall angle cones by SPIF. The same material was deep drawn and a bulge test part was formed to compare with SPIF. Moreover, the formed parts were sectioned and characterized for texture and surface finish at equivalent strains. To compare the strain paths of SPIF and deep drawing, finite element models were used [52]. For AA 1050 sheet metal, the deformation characteristics, forming behavior, and deformation mechanism of the SPIF process were evaluated. For process deformation characteristics such as dimensional accuracy, thickness distribution, true surface strain, von Mises stress, and equivalent plastic strain, evolved at different forming stages, were estimated through experimental investigation and finite element analysis. Analysis was carried out to identify the reason of typical failure under biaxial strain mode [53].

5. Aluminum alloy behavior during hydroforming process

The metal forming process in which a pressurized fluid either plastically deforms or aids in deforming a given blank material (sheet or tube) into a desired shape as depicted is a hydroforming process. **Figure 4** indicates the complete process. Using this process, more complex shapes with more strength and low cost can be manufactured as compared with stamping, forging, or casting processes [54].

Tube hydroforming process on different aluminum alloys is discussed in the following sections. At different temperatures, tube hydroforming analysis of aluminum alloy AA1050 was studied and the effect of temperature on thickness distribution of the final product was investigated. Also, for evaluating numerical results, a warm hydroforming set-up had been designed and manufactured. Conferring to numerical and experimental results in the case of free bulging, increase of the process temperature causes more uniform thickness distribution which leads to better material formability. A viscoplastic model was developed to consider the influence of microscopic evolution and macroscopic deformation to represent the deformation behavior of aluminum alloy sheet AA7075-O in the warm hydroforming process. By using the pressure rate, the evolution of dislocation density and kinematic isotropic hardening on a hydroforming environment, a set of rate dependent constitutive equations was constructed and proposed to predict stress-strain response of the material. The hydraulic bulge experiments on aluminum alloy at warm temperature indicated that the deformation behavior of the material was more sensitive to pressure rate. To determine the optimum values of a set of free material constants associated with the proposed constitutive model, the genetic algorithm optimization technique was used. The computed data were in good agreement with the test data on the basis of the optimized material constants [55, 56].

Friction stir welding (FSW) tube of 2024-O aluminum alloy rolled plates was coiled and produced by processing sequence. The plastic deformation characteristics were investigated experimentally and numerically during hydroforming with two types of end conditions. The performance of the FSW tubes was investigated by die-bulge forming with fixed ends. The wrinkling behavior during hydroforming was analyzed by employing axial feed on the tube ends. Severe thinning was observed at one quarter of the expansion zone from symmetry plane. Along the hoop direction, the base material near the weld observed a severe thinning. The thickness distribution greatly depends on the sequence of the contacting die and the variations of the curvature radius of the tube during hydroforming. Moreover, the weld shows an inhibitory effect for the generation of the wrinkles and decreases the number of the wrinkles as compared to the seamless tube during hydroforming [57].

An experimental and numerical simulation was studied on 6063-T4 aluminum alloy cross member through the hydroforming process. Severe thinning and

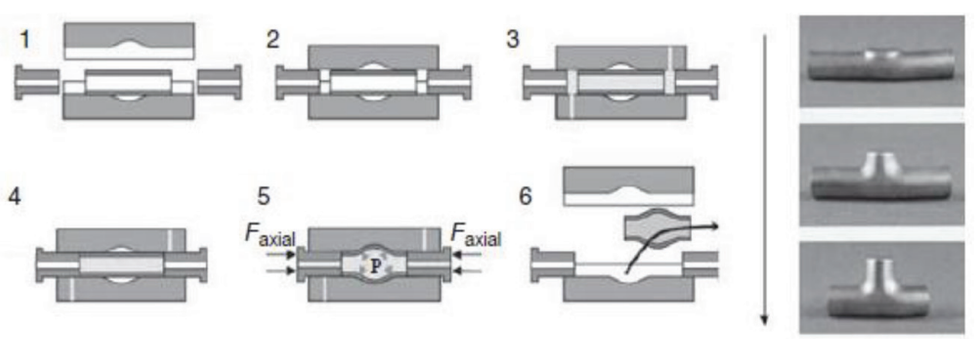

Figure 4.
Steps in a typical hydroforming process shown on a small tubular part [54].

bursting were avoided during hydroforming, composite design method was carried out, and the significance of pre-form structural parameters was discussed on thinning. An experimental research was conducted on thickness distribution of typical sectional profiles and dimension accuracy as per the optimum pre-form shape.

FEM simulations and experiments were conducted on the formability of aluminum alloy AA2024-O. The effects of strain rate on the formability during the active hydroforming process were investigated. Results indicated that aluminum alloy AA2024-O is not sensitive to pressure rate at room temperature. Furthermore, the deformation capacity of aluminum alloys can be improved effectively, and more uniform distribution of wall thickness can be obtained. The wrinkling behavior and thickness distribution of 5A06 aluminum alloy sheets in an annealed state was investigated numerically and experimentally under different hydraulic pressures in the hydroforming of single-layer and double-layer sheets. The upper, thicker sheet synchronously deforms with the lower, thinner sheet during hydroforming. When the double-layer sheets were separated, a thinner curved sheet part will be manufactured. From the simulation and experimental results, the upper, thicker sheet was effectively suppressing the wrinkles of the lower, thinner sheet and improved the thickness distribution. This was due to the increasing anti-wrinkle ability of the formed sheet and the interfacial friction between the double-layer sheets. In addition, the maximum hydraulic pressure was decreased via hydroforming of double-layer sheets. This method reduced the drawing force for large sheet parts and meets the requirement of energy conservation [58–60].

A specialized hydroforming process set-up was designed for 2A12 aluminum alloy curved shell double-sided sheet. The influence of double-sided liquid pressure on the thickness distribution was evaluated. The thickness distribution of the formed shells was measured and compared under different loading paths. Using simulation analysis, the deformation mode and the stress state were analyzed to understand the mechanism of the thickness variation. It was shown that the forward pressure plays a negative role in the thickness distribution of the formed parts. The deformation mode of the shells varies slightly when forward pressures are added. The Von Mises stress and the effective strain of the components were improved when conducting the double-sided hydroforming process. The larger thinning phenomenon was noted by adding forward pressure and by increasing reduced third principle stress on the blank. Through a steam hydroforming process, an experimental formability study was carried out on aluminum sheet 2017A. The steam hydroforming process takes advantage of the coupling between the thermal and mechanical loads applied. The variation of the supplied electrical power on the hydroforming temperature and steam pressure effects was studied. The evolution of strains and stresses in metal sheets was analyzed. The experimental results showed that the supplied electrical power increases the heating rate and has no effect on bursting temperature or pressure. Furthermore, the evolution of the vapor pressure as a function of temperature was independent of the supplied electrical power and the deformation in the thin sheets under the steam pressure decreases the stress flow and raises the plastic deformation [61, 62].

Using elliptical bulging dies under various temperatures and pressure rates, warm/hot sheet bulging tests were conducted on 2A16-O aluminum alloy. The macroscopic and microscopic influence of the pressure rate on the formability and microstructural evolution of hydrobulging parts during warm/hot sheet hydroforming was investigated. The results revealed that the forming limit of the aluminum alloy was influenced by the pressure rate as the temperature rose, wherein a lower pressure rate resulted in a higher forming limit. This study demonstrated that warm/hot sheet hydroforming of aluminum alloy may lead to an improved forming limit and inhibit microstructural degradation during processing [63]. A

hydroforming analysis was made on extruded aluminum tubular specimen made up of AA 6063 alloy bulged from the diameter of 38–54 mm. The thickness distribution at bulging the region along lateral and longitudinal directions was analyzed. The parameters considered are axial feed, tube thickness, fluid pressure, and die semi-cone angle. The forming characteristics such as thickness distribution and bulged diameter were studied using toolmaker microscope and coordinate measuring machine. Maximum shear thinning is observed in the largest diameter of the bulged portion of the tube [64].

6. Aluminum alloy behavior during bi-axial forming

Here, some of the recent discussions are made based on the bi-axial forming process. It is also treated as a stretching process in which sheet material experiences the tensile load along plane direction in the same time.

Biaxial warm forming behavior in the temperature range 200–350°C was investigated for three aluminum sheet alloys: Al 5754, Al 5182, and Al 6111-T4. The formability for all the three alloys improved at elevated temperatures; the strain hardened alloys Al 5754 and Al 5182 showed considerably greater improvement than the precipitation hardened alloy Al 6111-T4. Formability was studied by forming rectangular parts at a rapid rate using internally heated punch and die in both isothermal and nonisothermal conditions. The temperature effect on drawing of the sheet was found to have a large effect on formability. FLD under warm forming conditions was also determined, which showed results that are consistent with the evaluation of part depth. Biaxial forming behavior was investigated for three aluminum sheet alloys of Al 5182, Al 5754, and 6111-T4 using a heated die and punch in the warm forming temperature range of 200–350°C. It was found that all three alloys exhibited significant improvement in the formability compared with that at room temperature. The nonheat-treatable alloys of AA 5182 and AA 5754 showed a higher part depth than that of heat-treatable 6111-T4. The formidability characteristic was dependent on the blank holding pressure (BHP). When the BHP decreased, the formability increased, but increasing the forming temperature and/or BHP minimizes the wrinkling tendency and improves the forming performance. By increasing temperature and BHP, the stretchability of the sheet alloys was increased. Through setting the temperature 50°C higher than the punch temperature to enhance the drawing component, the optimum formability was achieved. Strain distribution was also improved with setting the die temperature higher than the punch temperature in a part in such a manner that postpones necking and fracture by altering the location of the greatest thinning [65].

The Gurson-Tvergaard-Needleman (GTN) damage model combined with the finite element method was used to investigate the influence of double-sided pressure on the deformation behavior of biaxially stretched AA6111-T4 sheet metal. The Marciniak-Kuczynski (M-K) localized necking model was used to predict the right-hand side of the forming limit diagram (FLD) of sheet metal under superimposed double-sided pressure. The forming limit curve (FLC) of the biaxially stretched AA6111-T4 sheet metal under the superimposed double-sided pressure had improved and the fracture locus shifts to the left. Besides, the formability increase value is sensitive to the strain path [66].

Through the numerical biaxial tensile tests of the sheet, the biaxial tensile deformation behavior of 5182 aluminum alloy sheet was predicted. From the numerical simulations, the stress-strain curves and the shapes of the contours of plastic work were calculated and were quantitatively verified by the experimental biaxial tensile test using the cruciform specimen. Using the results of experimental and numerical

biaxial tensile tests, parameters of the Yld2000-2d yield function were identified. Von Mises's and Hill's yield functions were identified using the experimental data and were compared. The simulation results confirmed that the forming simulation using the Yld2000-2d yield function identified by the numerical biaxial tensile tests was better than that of the Mises's and Hill's yield functions and was comparable to that of the Yld2000-2d yield function calibrated experimentally [67].

The forming limit strains at fracture for aluminum alloy 5086 were determined using an in-plane biaxial tensile test with a cruciform specimen. To identify the onset of fracture and the forming limit strains, a method based on the evolution of strain in the central area of the specimen and the observation of the macroscopic image of specimen surface was proposed. The forming limit strains at fracture were determined under different strain paths provided by the two independent axes of the experimental device. Finite element simulations were performed to determine and compare numerical forming limit strains with three ductile fracture criteria [68]. Warm temperature biaxial tension test apparatus was developed to achieve stress ratio and strain rate controls simultaneously. The warm temperature biaxial tension tests were conducted on AA5182-O aluminum alloy sheet with the thickness of 1 mm. The obtained results showed that the shapes of equi-plastic work loci did not have strong temperature dependency [69].

7. Summary

Forming behavior of different aluminum alloys is discussed in the above sections. The forming processes considered included the hot forming process, deep drawing process, incremental process, hydroforming process, and bi-axial forming. The effect of their parameters on aluminum alloys is realized. From each forming process and test, the forming limit strain is determined to quantify the formidability of each aluminum alloy. Moreover, the quantification of the formability of Al alloys can help the industries.

Author details

Perumalla Janaki Ramulu
Program of Mechanical Design and Manufacturing Engineering, School of Mechanical, Chemical and Materials Engineering, Adama Science and Technology University, Adama, Ethiopia

*Address all correspondence to: perumalla.janaki@astu.edu.et

References

[1] Cavaliere P. Hot and warm forming of 2618 aluminium alloy. Journal of Light Metals. 2002;**2**(4):247-252. DOI: 10.1016/S1471-5317(03)00008-7

[2] El-Danaf EA, AlMajid AA, Soliman MS. Hot deformation of AA6082-T4 aluminum alloy. Journal of Materials Science. 2008;**43**(18):6324. DOI: 10.1007/s10853-008-2895-4

[3] Jin N, Zhang H, Han Y, Wu W, Chen J. Hot deformation behavior of 7150 aluminum alloy during compression at elevated temperature. Materials Characterization. 2009;**60**(6):530-536. DOI: 10.1016/j.matchar.2008.12.012

[4] Huang X, Zhang H, Han Y, Wu W, Chen J. Hot deformation behavior of 2026 aluminum alloy during compression at elevated temperature. Materials Science and Engineering A. 2010;**527**(3):485-490. DOI: 10.1016/j.msea.2009.09.042

[5] Rokni MR, Zarei-Hanzaki A, Roostaei AA, Abedi HR. An investigation into the hot deformation characteristics of 7075 aluminum alloy. Materials and Design. 2011;**32**(4):2339-2344. DOI: 10.1016/j.matdes.2010.12.047

[6] Liu W, Zhao H, Li D, Zhang Z, Huang G, Liu Q. Hot deformation behavior of AA7085 aluminum alloy during isothermal compression at elevated temperature. Materials Science and Engineering A. 2014;**596**:176-182. DOI: 10.1016/j.msea.2013.12.012

[7] Yan J, Pan QL, Li B, Huang ZQ, Liu ZM, Yin ZM. Research on the hot deformation behavior of Al-6.2 Zn-0.70 Mg-0.3 Mn-0.17 Zr alloy using processing map. Journal of Alloys and Compounds. 2015;**632**:549-557. DOI: 10.1016/j.jallcom.2015.01.228

[8] Li H, Li Z, Song M, Liang X, Guo F. Hot deformation behavior and microstructural evolution of Ag-containing 2519 aluminum alloy. Materials and Design. 2010;**31**(4):2171-2176. DOI: 10.1016/j.matdes.2009.10.061

[9] Wang L, Yu H, Lee Y, Kim HW. Hot tensile deformation behavior of twin roll casted 7075 aluminum alloy. Metals and Materials International. 2015;**21**(5):832-841. DOI: 10.1007/s12540-015-5093-3

[10] Rajamuthamilselvan M, Ramanathan S. Hot deformation behaviour of 7075 alloy. Journal of Alloys and Compounds. 2011;**509**(3):948-952. DOI: 10.1016/j.jallcom.2010.09.139

[11] Bariani PF, Bruschi S, Ghiotti A, Michieletto F. Hot stamping of AA5083 aluminium alloy sheets. CIRP Annals-Manufacturing Technology. 2013;**62**(1):251-254. DOI: 10.1016/j.cirp.2013.03.050

[12] Fan X, He Z, Yuan S, Zheng K. Experimental investigation on hot forming-quenching integrated process of 6A02 aluminum alloy sheet. Materials Science and Engineering A. 2013;**573**:154-160. DOI: 10.1016/j.msea.2013.02.058

[13] Fan X, He Z, Yuan S, Lin P. Investigation on strengthening of 6A02 aluminum alloy sheet in hot forming-quenching integrated process with warm forming-dies. Materials Science and Engineering A. 2013;**587**:221-227. DOI: 10.1016/j.msea.2013.08.059

[14] Chen G, Chen M, Wang N, Sun J. Hot forming process with synchronous cooling for AA2024 aluminum alloy and its application. The International Journal of Advanced Manufacturing Technology. 2016;**86**(1-4):133-139. DOI: 10.1007/s00170-015-8170-3

[15] Wang A, Zhong K, El Fakir O, Liu J, Sun C, Wang LL, et al.

Springback analysis of AA5754 after hot stamping: Experiments and FE modelling. The International Journal of Advanced Manufacturing Technology. 2017;**89**(5-8):1339-1352. DOI: 10.1007/s00170-016-9166-3

[16] Fan XB, He ZB, Zhou WX, Yuan SJ. Formability and strengthening mechanism of solution treated Al-Mg-Si alloy sheet under hot stamping conditions. Journal of Materials Processing Technology. 2016;**228**:179-185. DOI: 10.1016/j.jmatprotec.2015.10.016

[17] Liu Y, Zhu Z, Wang Z, Zhu B, Wang Y, Zhang Y. Formability and lubrication of a B-pillar in hot stamping with 6061 and 7075 aluminum alloy sheets. Procedia Engineering. 2017;**207**:723-728. DOI: 10.1016/j.proeng.2017.10.819

[18] Kim JH, Lee CJ, Lee SB, Ko DC, Kim BM. Integrated hot forming and heat treatment process on Al6061 tailor rolled blank. International Journal of Precision Engineering and Manufacturing. 2017;**18**(1):127-132. DOI: 10.1007/s12541-017-0016-5

[19] Liu X, El Fakir O, Meng L, Sun X, Li X, Wang L. Effects of lubricant on the IHTC during the hot stamping of AA6082 aluminium alloy: Experimental and modelling studies. Journal of Materials Processing Technology. 2018;**255**:175-183. DOI: 10.1016/j.jmatprotec.2017.12.013

[20] Boljanovic V. Sheet Metal Forming Processes and Die Design. South Norwalk, CT: Industrial Press Inc; 2004

[21] Pourboghrat F, Venkatesan S, Carsley JE. LDR and hydroforming limit for deep drawing of AA5754 aluminum sheet. Journal of Manufacturing Processes. 2013;**15**(4):600-615. DOI: 10.1016/j.jmapro.2013.04.003

[22] Panicker SS, Prasad KS, Basak S, Panda SK. Constitutive behavior and deep drawability of three aluminum alloys under different temperatures and deformation speeds. Journal of Materials Engineering and Performance. 2017;**26**(8):3954-3969. DOI: 10.1007/s11665-017-2837-x

[23] Panicker SS, Singh HG, Panda SK, Dashwood R. Characterization of tensile properties, limiting strains, and deep drawing behavior of AA5754-H22 sheet at elevated temperature. Journal of Materials Engineering and Performance. 2015;**24**(11):4267-4282. DOI: 10.1007/s11665-015-1740-6

[24] Wang BY, Lei FU, Jing ZH, Huang MD. Effect of friction coefficient in deep drawing of AA6111 sheet at elevated temperatures. Transactions of Nonferrous Metals Society of China. 2015;**25**(7):2342-2351. DOI: 10.1016/S1003-6326(15)63849-3

[25] Xiao WC, Wang BY, Kang Y, Ma WP, Tang XF. Deep drawing of aluminum alloy 7075 using hot stamping. Rare Metals. 2017;**36**(6):485-493. DOI: 10.1007/s12598-017-0919-4

[26] Ma WY, Wang BY, Zhou J, Huang MD. Influence of process parameters on deep drawing of AA6111 aluminum alloy at elevated temperatures. Journal of Central South University. 2015;**22**(4):1167-1174. DOI: 10.1007/s11771-015-2630-7

[27] Kitayama S, Natsume S, Yamazaki K, Han J, Uchida H. Numerical investigation and optimization of pulsating and variable blank holder force for identification of formability window for deep drawing of cylindrical cup. The International Journal of Advanced Manufacturing Technology. 2016;**82**(1-4):583-593. DOI: 10.1007/s00170-015-7385-7

[28] Piccininni A, Di Michele G, Palumbo G, Sorgente D, Tricarico L. Improving the hydromechanical deep-drawing process using aluminum tailored heat treated blanks. Acta

Metallurgica Sinica. 2015;**28**(12):1482-1489. DOI: 10.1007/s40195-015-0347-0

[29] Dwivedi R, Agnihotri G. Numerical simulation and experimental analysis on the deep drawing of cylindrical cups. Transactions of the Indian Institute of Metals. 2015;**68**(1):31-34. DOI: 10.1007/s12666-015-0598-5

[30] Liu ZY, Xiong BQ, Li XW, Yan LZ, Li ZH, Zhang YA, et al. Deep drawing of 6A16 aluminum alloy for automobile body with various blank-holder forces. Rare Metals. 2018;**37**:1-8. DOI: 10.1007/s12598-018-1146-3

[31] Abbadeni M, Zidane I, Zahloul H, Fatu A, Hajjam M. Finite element analysis of fluid-structure interaction in the hydromechanical deep drawing process. Journal of Mechanical Science and Technology. 2017;**31**(11):5485-5491. DOI: 10.1007/s12206-017-1043-y

[32] Wang B, Wang GF, Jiang SS, Zhang KF. Effect of pulse current on thermal performance and deep drawing of SiCp/2024Al composite sheet. The International Journal of Advanced Manufacturing Technology. 2013;**67**(1-4):623-627. DOI: 10.1007/s00170-012-4510-8

[33] Pranavi U, Reddy PV, Lavanya K, Charyulu NN, Ramulu PJ. Effect of mechanical properties on deep drawing formability prediction. International Journal of Current Engineering and Technology. 2014;**2**:303-305. DOI: 10.14741/ijcet/spl.2.2014.5

[34] Pranavi U, Ramulu PJ, Chandramouli C, Govardhan D, Prasad PR. Formability analysis of aluminum alloys through deep drawing process. In: IOP Conference Series: Materials Science and Engineering. Vol. 149. IOP Publishing; 2016. p. 012025. DOI: 10.1088/1757-899X/149/1/012025

[35] Reddy PV, Ramulu PJ, Madhuri GS, Govardhan D, Prasad PR. Design and analysis of deep drawing process on angular deep drawing dies for different anisotropic materials. In: IOP Conference Series: Materials Science and Engineering. Vol. 149. IOP Publishing; 2016. p. 012142. DOI: 10.1088/1757-899X/149/1/012142

[36] Ramulu PJ, Rao PS, Yimer W. Springback analysis on AA 6061 aluminum alloy sheets. In: AIP Conference Proceedings. Vol. 1769. AIP Publishing; 2016. p. 200023. DOI: 10.1063/1.4963641

[37] Reddy PV, Ramesha J, Rao PS, Ramulu PJ. Experimental and numerical analysis on deep drawing rectangular cups made of different anisotropic materials. Materials Today: Proceedings. 2018;**5**(13):27171-27177. DOI: 10.1016/j.matpr.2018.09.028

[38] Jackson K, Allwood J. The mechanics of incremental sheet forming. Journal of Materials Processing Technology. 2009;**209**(3):1158-1174. DOI: 10.1016/j.jmatprotec.2008.03.025

[39] Park JJ, Kim YH. Fundamental studies on the incremental sheet metal forming technique. Journal of Materials Processing Technology. 2003;**140**(1-3):447-453. DOI: 10.1016/S0924-0136(03)00768-4

[40] Golovashchenko S, Krause A. Improvement of formability of 6xxx aluminum alloys using incremental forming technology. Journal of Materials Engineering and Performance. 2005;**14**(4):503-507. DOI: 10.1361/105994905X56133

[41] Hussain G, Gao L, Hayat N, Dar NU. The formability of annealed and pre-aged AA-2024 sheets in single-point incremental forming. The International Journal of Advanced Manufacturing Technology. 2010;**46**(5-8):543-549. DOI: 10.1007/s00170-009-2120-x

[42] Liu Z, Li Y, Meehan PA. Experimental investigation of

mechanical properties, formability and force measurement for AA7075-O aluminum alloy sheets formed by incremental forming. International Journal of Precision Engineering and Manufacturing. 2013;**14**(11):1891-1899. DOI: 10.1007/s12541-013-0255-z

[43] Mugendirana V, Gnanavelbabub A. Comparison of FLD and thickness distribution on AA5052 aluminium alloy formed parts by incremental forming process. Procedia Engineering. 2014;**97**:1983-1990. DOI: 10.1016/j.proeng.2014.12.353

[44] Do VC, Nguyen DT, Cho JH, Kim YS. Incremental forming of 3D structured aluminum sheet. International Journal of Precision Engineering and Manufacturing. 2016;**17**(2):217-223. DOI: 10.1007/s12541-016-0028-6

[45] Alinaghian I, Ranjbar H, Beheshtizad MA. Forming limit investigation of aa6061 friction stir welded blank in a single point incremental forming process: RSM approach. Transactions of the Indian Institute of Metals. 2017;**70**(9):2303-2318. DOI: 10.1007/s12666-017-1093-y

[46] Amini S, Gollo AH, Paktinat H. An investigation of conventional and ultrasonic-assisted incremental forming of annealed AA1050 sheet. The International Journal of Advanced Manufacturing Technology. 2017;**90**(5-8):1569-1578. DOI: 10.1007/s00170-016-9458-7

[47] Pacheco PA, Silveira ME. Numerical simulation of electric hot incremental sheet forming of 1050 aluminum with and without preheating. The International Journal of Advanced Manufacturing Technology. 2018; **94**(9-12):3097-3108. DOI: 10.1007/s00170-017-0879-8

[48] Kumar A, Gulati V, Kumar P, Singh V, Kumar B, Singh H. Parametric effects on formability of AA2024-O aluminum alloy sheets in single point incremental forming. Journal of Materials Research and Technology. 2018;**8**(1):1461-1469. DOI: 10.1016/j.jmrt.2018.11.001

[49] Mugendiran V, Gnanavelbabu A. Analysis of hole flanging on AA5052 alloy by single point incremental forming process. Materials Today: Proceedings. 2018;**5**:8596-8603

[50] Barnwal VK, Chakrabarty S, Tewari A, Narasimhan K, Mishra SK. Forming behavior and microstructural evolution during single point incremental forming process of AA-6061 aluminum alloy sheet. The International Journal of Advanced Manufacturing Technology. 2018;**95**(1-4):921-935. DOI: 10.1007/s00170-017-1238-5

[51] Li Z, Lu S, Zhang T, Zhang C, Mao Z. 1060 Al electric hot incremental sheet forming process: Analysis of dimensional accuracy and temperature. Transactions of the Indian Institute of Metals. 2018;**71**(4):961-970. DOI: 10.1007/s12666-017-1229-0

[52] Nath M, Shin J, Bansal A, Banu M, Taub A. Comparison of texture and surface finish evolution during single point incremental forming and formability testing of AA 7075. In: TMS Annual Meeting & Exhibition. Cham: Springer; 2018. pp. 225-232. DOI: 10.1007/978-3-319-72284-9_31

[53] Shrivastava P, Tandon P. Microstructure and texture-based analysis of forming behavior and deformation mechanism of AA1050 sheet during single point incremental forming. Journal of Materials Processing Technology. 2019;**266**:292-310. DOI: 10.1016/j.jmatprotec.2018.11.012

[54] Koç M, editor. Hydroforming for Advanced Manufacturing. Woodhead

Publishing; 2008. https://www.elsevier.com/books/hydroforming-for-advanced-manufacturing/koc/978-1-84569-328-2

[55] Hashemi SJ, Naeini HM, Liaghat G, Tafti RA, Rahmani F. Numerical and experimental investigation of temperature effect on thickness distribution in warm hydroforming of aluminum tubes. Journal of Materials Engineering and Performance. 2013;**22**(1):57-63. DOI: 10.1007/s11665-012-0213-4

[56] Lang L, Du P, Liu B, Cai G, Liu K. Pressure rate controlled unified constitutive equations based on microstructure evolution for warm hydroforming. Journal of Alloys and Compounds. 2013;**574**:41-48. DOI: 10.1016/j.jallcom.2013.03.134

[57] Hu ZL, Wang XS, Pang Q, Huang F, Qin XP, Yuan SJ, et al. Experimental and numerical study on hydroforming characteristics of friction stir welded aluminum alloy tubes. The International Journal of Advanced Manufacturing Technology. 2015;**80**(5-8):959-969. DOI: 10.1007/s00170-014-6613-x

[58] Kong D, Lang L, Sun Z, Ruan S, Gu S. A technology to improve the formability of thin-walled aluminum alloy corrugated sheet components using hydroforming. The International Journal of Advanced Manufacturing Technology. 2016;**84**(1-4):737-748. DOI: 10.1007/s00170-015-7727-5

[59] Zhou BJ, Xu YC. Wrinkle behavior of hydroforming of aluminum alloy double-layer sheets. Journal of Metals. 2016;**68**(12):3201-3207. DOI: 10.1007/s11837-016-2025-8

[60] Cai Y, Wang XS, Yuan SJ. Pre-form design for hydro-forming of aluminum alloy automotive cross members. The International Journal of Advanced Manufacturing Technology. 2016;**86**(1-4):463-473. DOI: 10.1007/s00170-015-8160-5

[61] Liu W, Chen YZ, Yuan SJ. Mechanism analysis on thickness distribution of aluminum alloy hemispherical shells in double-sided sheet hydroforming. The International Journal of Advanced Manufacturing Technology. 2017;**89**(5-8):2011-2020. DOI: 10.1007/s00170-016-9248-2

[62] Aissa S, Mohamed S, Tarek L. Experimental study of steam hydroforming of aluminum sheet metal. Experimental Techniques. 2017;**41**(5):525-533. DOI: 10.1007/s40799-017-0191-4

[63] Cai G, Wu C, Gao Z, Lang L, Alexandrov S. Investigation on the effect of pressure rate on formability of aluminum alloy during warm/hot sheet hydroforming. AIP Advances. 2018;**8**(9):095313. DOI: 10.1063/1.5050222

[64] Selvakumar AS, Rajan BS, Balaji MS, Selvaraj B. Strain analysis of AA6063 aluminum alloy by tube hydroforming process. In: Advances in Manufacturing Processes. Singapore: Springer; 2019. pp. 13-21. DOI: 10.1007/978-981-13-1724-8_2

[65] Li D, Ghosh AK. Effects of temperature and blank holding force on biaxial forming behavior of aluminum sheet alloys. Journal of Materials Engineering and Performance. 2004;**13**(3):348-360. DOI: 10.1361/10599490419225

[66] Liu J, Wang Z, Meng Q. Numerical investigations on the influence of superimposed double-sided pressure on the formability of biaxially stretched AA6111-T4 sheet metal. Journal of Materials Engineering and Performance. 2012;**21**(4):429-436. DOI: 10.1007/s11665-011-9941-0

[67] Yamanaka A, Hashimoto K, Kawaguchi J, Sakurai T, Kuwabara T.

Material modeling and forming simulation of 5182 aluminum alloy sheet using numerical biaxial tensile test based on homogenized crystal plasticity finite element method. Journal of Japan Institute of Light Metals. 2015;**65**:561-567

[68] Song X, Leotoing L, Guines D, Ragneau E. Investigation of the forming limit strains at fracture of AA5086 sheets using an in-plane biaxial tensile test. Engineering Fracture Mechanics. 2016;**163**:130-140. DOI: 10.1016/j.engfracmech.2016.07.007

[69] Hamasaki H, Tamashiro F. Biaxial deformation on AA5182-O aluminium alloy sheet at warm temperature. Journal of Physics: Conference Series. 2018;**1063**(1):012032. DOI: 10.1088/1742-6596/1063/1/012032